BEAM DYNAMICS CALCULATIONS FOR THE LAMPF OPTICALLY PUMPED ION SOURCE

R. J. Hayden and M. J. Jakobson
Physics and Astronomy, Univ. of Montana
Missoula, MT 59812

O. B. van Dyck and R. L. York
Los Alamos National Laboratory
Los Alamos, NM 87545

Summary

The space charge code SCHAR[1] has been used to interpret some of the measurements made with the LAMPF ECR source[2]. Calculations were made for rectangular hole (ribbon beam), single hole and multihole electrodes. Measured rotation of the plane of the ribbon beam in the constant solenoid field showed that when the polarizer cell was not utilized the beam was essentially not neutralized after it emerged from the extraction electrodes. There is evidence that when the polarizer cell is "turned on" the beam becomes neutralized from the polarizer back toward the electrode structure. The total measured current from single and multihole electrodes with the polarizer cell "on" is proportional to the area of the electrode apertures. Beam simulation calculations indicate that if the beam extracted from the source is uniform across the multihole structure, then in order for the perimeter holes to provide as much current per area, the beam would have to be at least partially neutralized after exiting from the electrode structure. POISSON calculated fields were used for the single and multihole electrode fields. For a ribbon beam the field used was that of a very long slit. The initial transverse velocity and energy of the beam at the entrance to the three electrodes were adjusted to provide agreement with the measured harp histograms. The energy of the ions leaving the (unmodeled) ECR plasma determines the current for a given electrode structure and voltage. Initial transverse velocity was not a sensitive parameter. Electrode radial fields and beam space charge forces generate most of the transverse velocities observed as the beam exits from the electrodes. "Tails" which were present in the measured harp data could be explained by an H_2^+ component in the beam. Alternate explanations for the "tails" were not explored. The measured dependence of the current on the middle electrode voltage could not be modeled without assuming beam neutralization which was dependent upon that voltage.

Ribbon Beams

One by eight mm rectangular aperture electrodes were inserted in the LAMPF source. Figure 1 is a schematic diagram of the source. Vertical and horizontal harps movable axially were used to measure the beam envelope in the constant solenoid field. In order to understand the rectangular beam behavior it is instructive to consider first the case of charged particles with negligible space charge, moving classically in a constant magnetic field B_0 which defines the direction of the Z-axis.

The projection of each particle's path upon a plane perpendicular to the z-axis is a circle of radius

$$R_\perp = \frac{mv_\perp}{qB_0}$$ where $v_\perp$ is the constant magnitude of the component of the velocity perpendicular to the z-axis. The time required to complete the circle is the cyclotron period $T = \frac{2\pi m}{qB_0}$ which is independent of $v_\perp$.

Thus if a group of particles comes through an orifice

in the plane z = 0 at time t = 0, then, at integral multiples of T, each particle will have returned to its original position in the perpendicular plane. The z position of particle k at its n'th return is

$$z_n = nTv_z(k)$$

where $v_z(k)$ is the z-component of the velocity of the kth particle. If v_z and m are the same for all particles, then an exact image of the distribution is obtained at each position z_n. As long as $n\Delta v_z \ll 1$, an approximate image will be formed at these positions. Δv_z is the maximum spread in v_z for the particles under consideration.
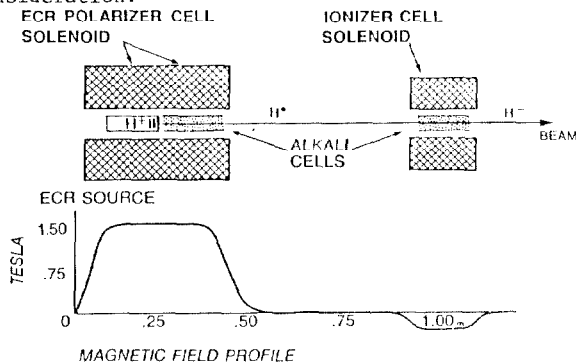

MAGNETIC FIELD PROFILE

Figure 1. Schematic of optically pumped polarized H⁻ ion source.

The effect of space charge is to provide an electric field perpendicular to the magnetic field. If the beam is initially a ribbon beam, at each focus the plane of the ribbon will be rotated with the rotation angle proportional to the current. A ribbon beam carrying a total charge/length σ_T at a speed v_z will represent a current $i = \sigma_T v_z$. If the charge filaments are distributed across a beam of dimensions 2a by 2b with a density $\sigma(x,y)$, then:

$$\sigma_T = \int_{-a}^{a} \int_0^{2b} \sigma(x,y)\,dy\,dx.$$

At a point y' on the y axis the force on a charge is qE_y. The contribution to E_y by $\sigma(x,y)dxdy$ is

$$dE_y = \frac{\sigma\sin\theta}{2\pi\varepsilon_0 r}\,dxdy \quad \text{where} \quad r^2 = x^2 + (y-y')^2 \quad \text{and}$$

$$\sin\theta = \frac{y'-y}{r}.$$

Integrating one obtains

$$E_y = \frac{i}{2\pi\varepsilon_0(y'-b)v_z} \frac{B-.5}{2A} \int_0^A \log\left(\frac{w^2 + B^2}{w^2+(1-B)^2}\right) dw \qquad (1)$$

with $A = a/2b$ and $B = y'/2b$.

For an edge particle with 2a = 1mm, and y' = 2b = 8mm, A = 1/16 and B = 1

$$E_y = \frac{i}{2\pi\varepsilon_o bv_z} \cdot 1.866. \qquad (2)$$

For 25 ma of 5.0 keV protons, $E_y = 2 \times 10^5$ volts/m.

The composite space charge electric field and solenoid magnetic field forces result in a rotation of the ribbon. Since the space charge forces are non-linear with respect to the distance from the center of the beam, after a number of focussing lengths the ribbon will generate "tails" and degenerate into a "blob". Figures 2 and 3 show the rotation and degeneration of a ribbon beam as calculated by SCHAR. Figure 4 is a plot of the angle of the ribbon as a function of axial distance. The estimated rotation obtained using the electric field of eq. (2) is in agreement with the SCHAR calculation. Measured harp data were in good agreement with harp data simulated by SCHAR. Particle motion is similar for a circular aperture but less obvious due to symmetry.
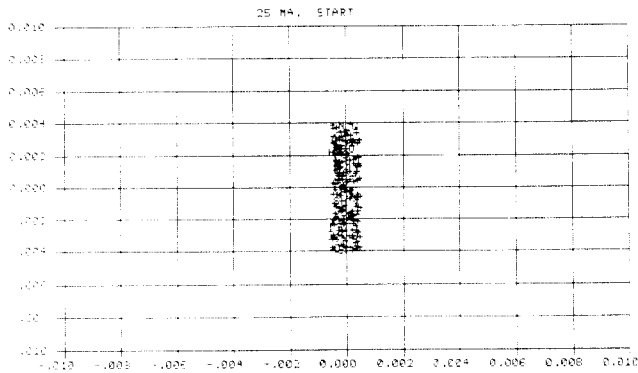
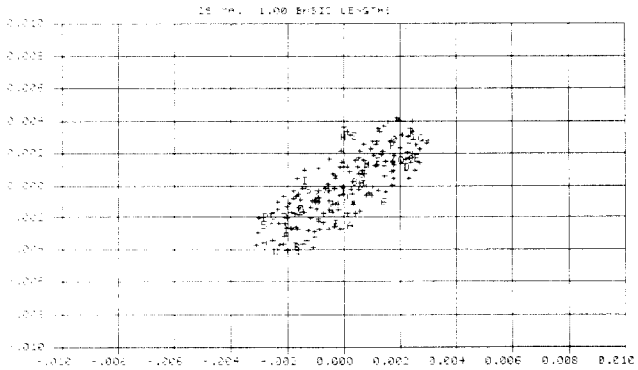

Figure 2.   Ribbon beam at exit of electrodes.

Figure 3.   Ribbon beam first focus.   Note ~35° rotation from Figure 2.
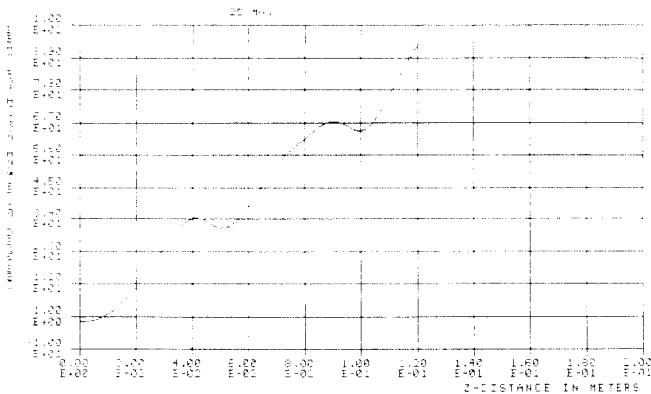

Figure 4.   Demonstrates the progressive ribbon rotation with axial distance.

Single and Multihole Electrodes

Sources studied were modeled as a series of parallel, equipotential plates. Beam induced charges on the plates were neglected. Initial studies used three electrodes of one mm thickness separated one mm. One, seven or thirteen 1.5 mm diameter holes with a minimum separation of .30 mm were in the different structures. For the multihole clusters, we used POISSON calculated fields and assumed the field due to each hole was independent of the other holes and was given by the single hole calculation. The motion of filaments in fields so calculated was very similar to the motion in another approximate model – a hole surrounded by a metal ring and annular gap. The general effect of the independent hole fields is to overestimate the magnitude of the radial fields. Various hole sizes, plate thicknesses and plate separations as well as a nineteen hole electrode were tried.

Extraction electrode studies were initiated by finding out what beam exiting the final electrode would reproduce the observed harp data. The three variable beam input parameters were current, maximum transverse velocity, and position-velocity correlation. The transverse velocity correlation parameter used in SCHAR measures whether the beam is converging or diverging as it emerges from the electrodes and is determined by the distance the first minimum in the harp data is from the electrodes. The magnitude of the assumed initial transverse velocity is determined by the variation in beam size as observed by the harp measurements. The axial separation of the minima in the harp data is somewhat dependent on the current and thus provides a check of the current measurement.

The next phase of the electrode studies was one in which the beam parameters at the entrance to the electrodes were adjusted to give the proper exit beam for the harp data. The initial beam was placed across the holes in a uniform statistical manner. All beam filaments were given the same initial speed. The components of the initial velocity perpendicular to the path were varied and both uniform statistical and parabolic statistical distributions were tried. Of these input parameters, the predominantly important one was the initial speed entering the electrodes. Typically that corresponds to the velocity resulting from the POISSON calculated electrical potential at the entrance to the electrode structure plus about 40 eV more. It determines the current through the apertures. In our modeling we set this at 1.6×10^5 m/sec, the value which gave the best fit to the measured 7 hole harp data for 5 keV protons. As an unneutralized beam emerges from the plasma, space charge forces dominate and make the beam diverging. Midway in the first electrode the radial inward electric forces dominate and cause the beam to be converging. Near the end of the second electrode the beam again becomes diverging due to space charge forces and the radial outward electrode forces. It was assumed that whenever a beam filament was passing through a hole in the metal only the current in that hole contributed to the space charge forces. Also, whenever the path of a filament contacted the walls of a plate it was lost and neglected in further calculations. Current loss on the second and third electrodes is a useful parameter for checking the calculation. In general, as the second electrode becomes more positive, the beam loss on the last electrode increases, the beam emittance decreases and the beam current diminishes.

When the current of the LAMPF source was measured as a function of the second electrode voltage, a peak current was observed with the electrode voltages 5 kV, -.2 kV and 0. When SCHAR was used to model the source there was a peak observed with the central electrode -200 V if the space charge was neutralized at the end

855

of the source but it was much smaller than the observed peak.

At prespecified positions beam profiles, x and y histograms of beam current, x emittance, x rms, V_x rms and the current with a specified emittance could be obtained from SCHAR. A comparison of the measured and calculated harp data at the second focus of the seven hole electrode structure is shown in Figure 5. The measured and calculated harp data for a number of points along the axis are in Figure 6.
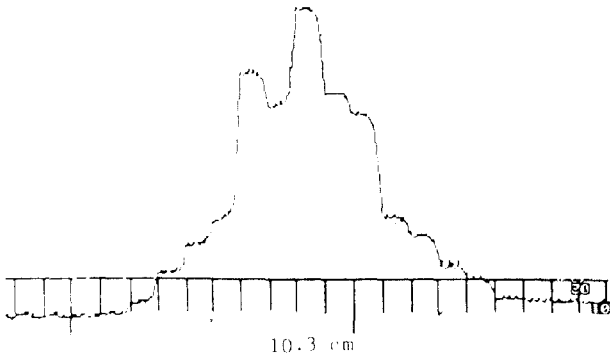
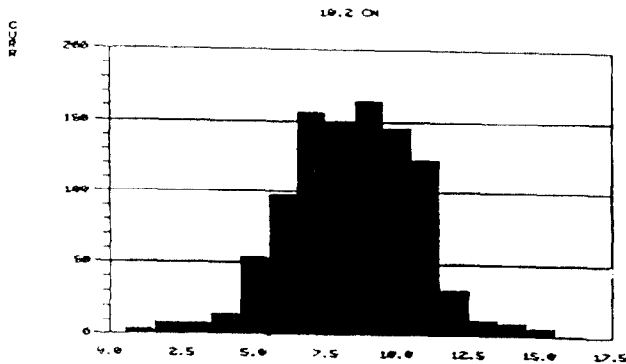

Figure 5(a). The measured harp histogram.

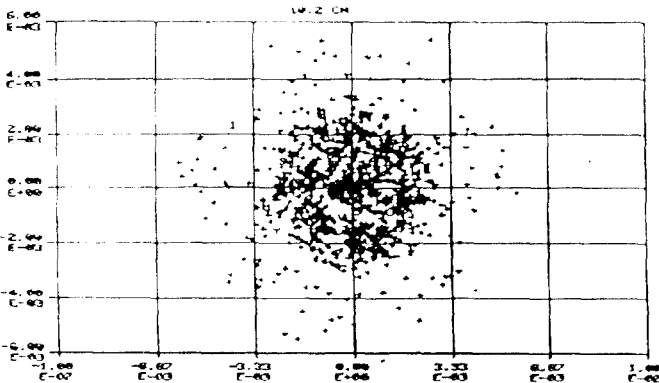Figure 5(b). The SCHAR calculated histogram.

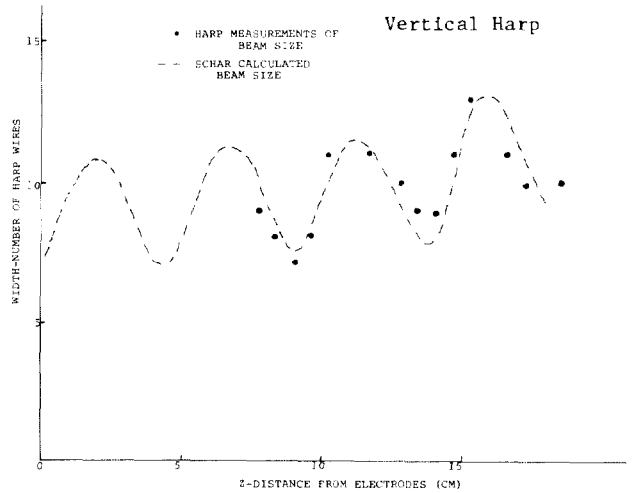Figure 5(c). The calculated transverse distribution for 19 ma of 5 keV protons.

Figure 6. Seven hole source beam size variation in the solenoid. The width at half height is plotted.

Results

None of the multihole electrode systems modeled with SCHAR was a factor of three better than the others in providing current with emittance less than 250 mm mr (non normalized @ 5 keV) for the polarizer cell. This emittance was arbitrarily selected as useful beam emittance for the purpose of comparing electrode structures. Although the total current at the polarizer cell is proportional to the total area of the holes, the emittance of the total beam increases approximately as the radius of the multihole structure so that the useful beam will not be proportional to source aperture area. The current entering a 7/16" diameter aperture at the ionizer cell is only about 1% of the source current – if the efficiency for $H^+ \rightarrow H^\circ$ conversion is 100%. The percentage of the beam retained can be increased by shaping the ECR source and polarizer cell magnetic field to make the beam focus at the ionizer cell[3]. However the transverse velocity from the source must be reduced an order of magnitude for the LAMPF-ECR source modeled in these studies in order for that method to provide a large increase in current.

References

1. M. J. Jakobson and R. J. Hayden, "Macrofilament Simulation of High Current Beam Transport," IEEE, NS 30 #4, p. 2540, 1983.

2. R. L. York, M. Dulick, W. D. Cornelius, O. B. van Dyck, "An Optically Pumped Polarized Ion Source for LAMPF," Proceedings of the International Workshop on Hadron Facility Technology, Feb. 1987.

3. R. J. Hayden and M. J. Jakobson, "Shaping Solenoid Fields to Reduce Emittance Degradation of Polarized H⁻ Ion Beams," Nuclear Instruments and Methods, (In Press).